

Supporting Information

Rapidly Gelled Lipoic Acid-based Supramolecular Hydrogel for 3D Printing of Adhesive Bandage

Jiujiang Zeng¹, Haowei Fang², Haiyang Pan², Huijie Gu^{3}, Kunxi Zhang^{1,2*}, Yanli Song^{1,*}*

¹ Department of Emergency, Tongji Hospital, School of Medicine, Tongji University, Shanghai 200065, P. R. China.

² Department of Polymer Materials, School of Materials Science and Engineering, Shanghai University, Shanghai, 200444, P.R. China.

³ Department of Orthopedics, Minhang Hospital, Fudan University, Shanghai, 201199, P.R. China.

* Corresponding authors:

Huijie Gu, Email: guhuijie0110@126.com

Kunxi Zhang, E-mail: zhangkunxi@shu.edu.cn

Yanli Song, E-mail: songyanli@tongji.edu.cn

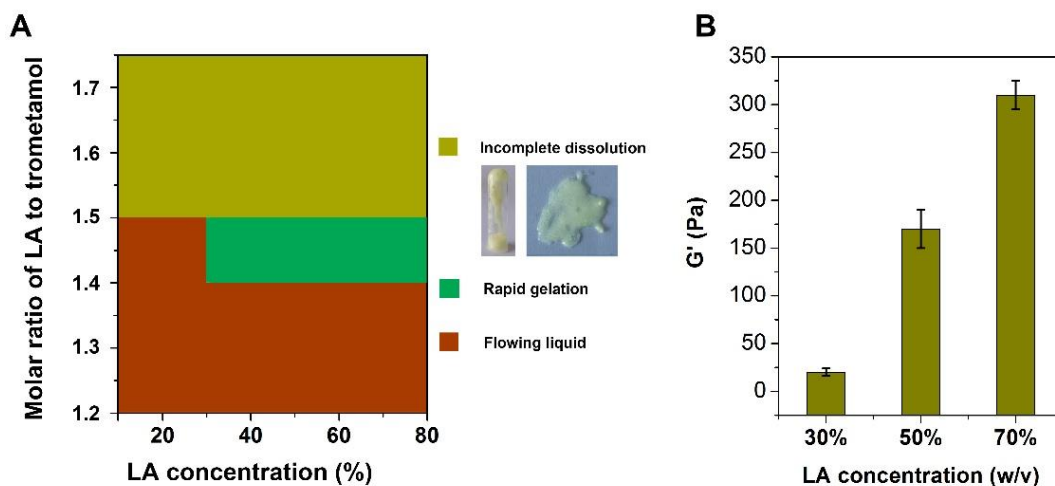


Figure S1. Effect of composition on rapid gelation and mechanical properties. (A) Effect of LA concentration and LA/Tris molar ratio on rapid gelation. (B) the effect of LA concentration on G' .

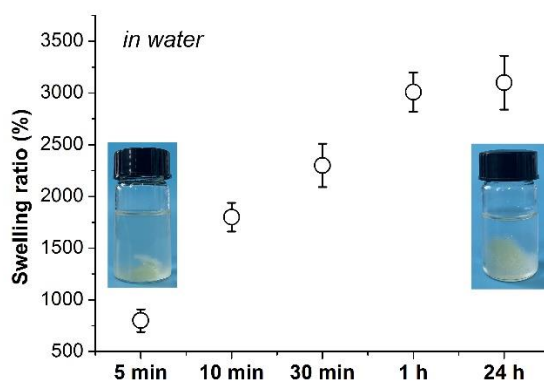


Figure S2. Swelling of the rapidly gelled hydrogel in water.

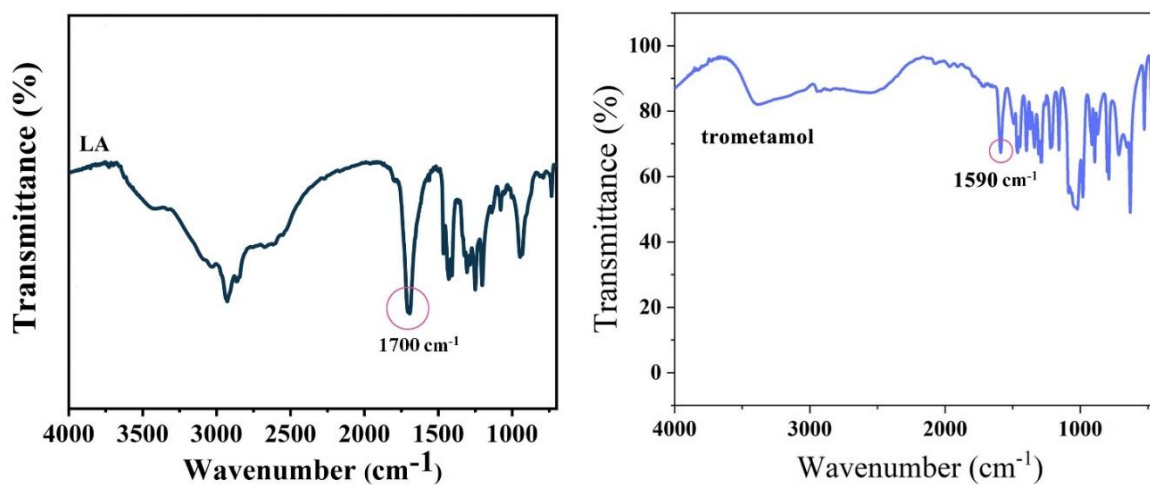


Figure S3. FT-IR spectrum of LA and Tris.

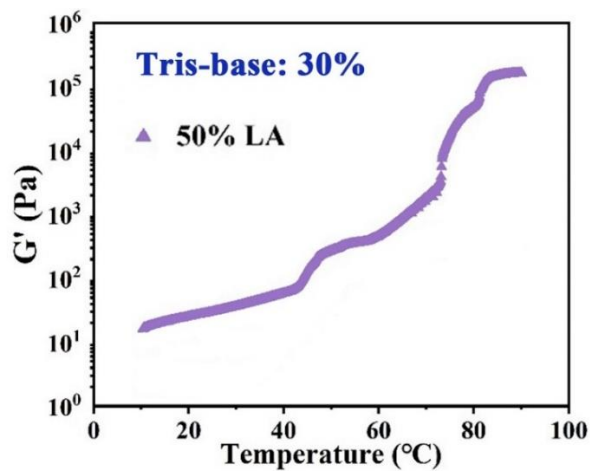


Figure S4. G' of PLA polymerized from LA solution with the LA concentration of 50% w/v and the Tris concentration of 30% w/v during heating.

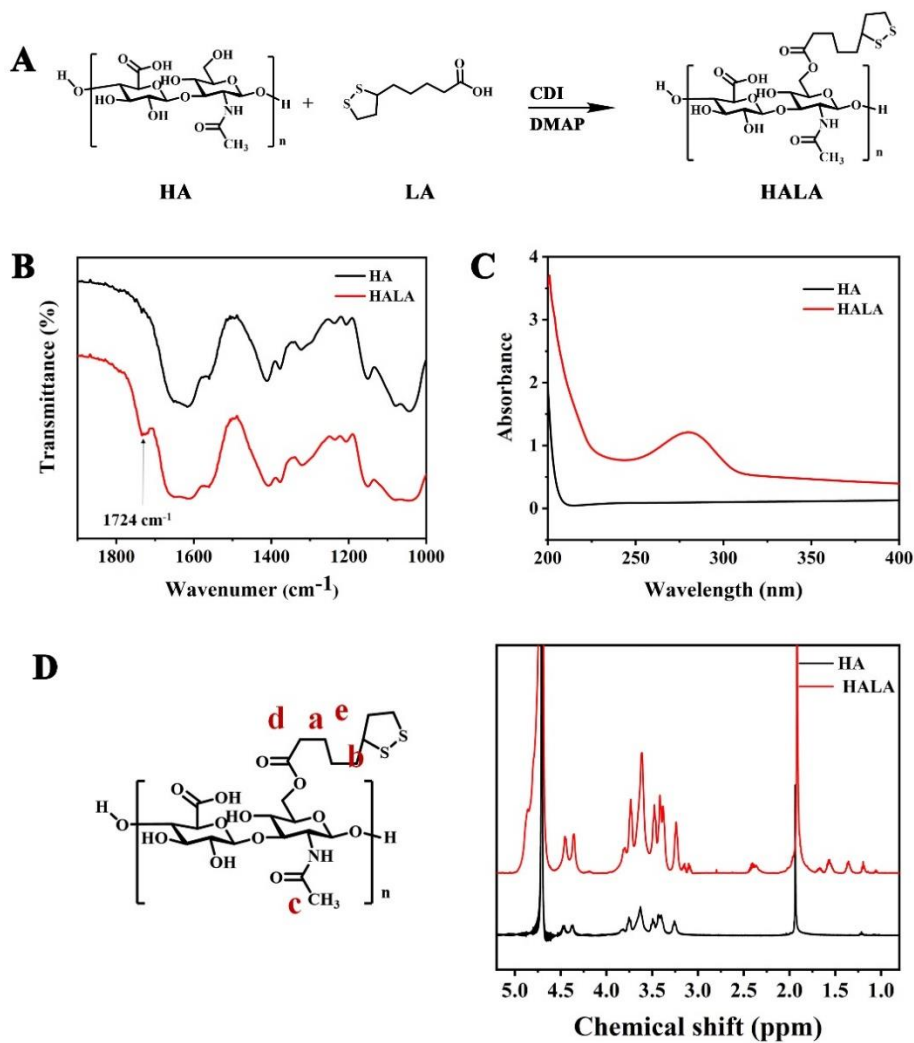


Figure S5. Characterization of HALA. (A) Synthesis of HALA. (B) FT-IR spectrum. (C) UV visible absorption spectrum. (D) ^1H NMR spectrum of HALA. Discussion: LA was grafted onto HA to synthesize HALA, which was used as a macromolecular crosslinker to co-polymerize with LA to form a crosslinked PLA-HA hydrogel (**Figure S5A**). The appearance of a typical characteristic peak of ester groups at 1724 cm^{-1} in FT-IR spectrum, as well as the appearance of a characteristic absorption peak of disulfide bonds at 280 nm in the UV-visible absorption spectrum confirmed the grafting of LA onto HA (**Figure S5B,C**). ^1H NMR spectrum further confirmed the synthesis of HALA (**Figure S5D**). The high grafting rate of LA would affect the solubility of HALA in water. Thus, HALA with the LA graft rate calculated from ^1H NMR of 2% was used in the present study.

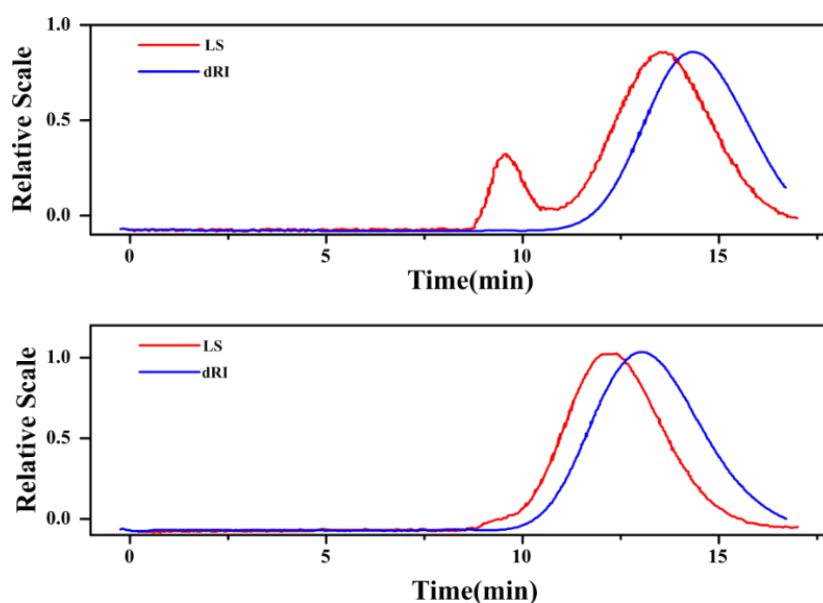


Figure S6. Molecular weight of HA before and after LA conjugation tested by GPC.

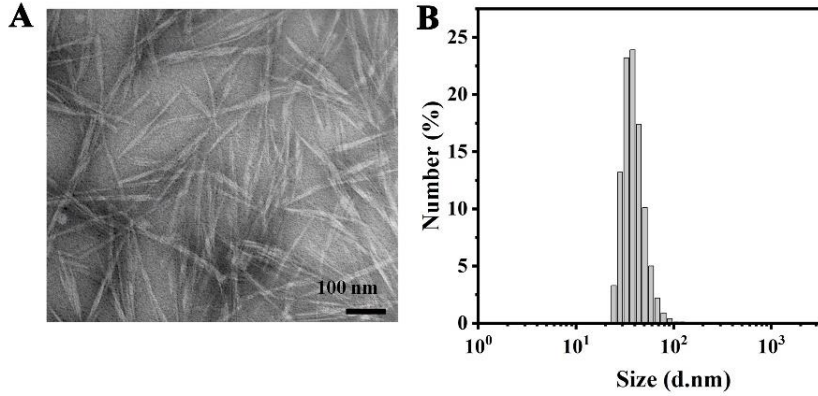
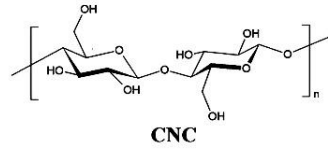
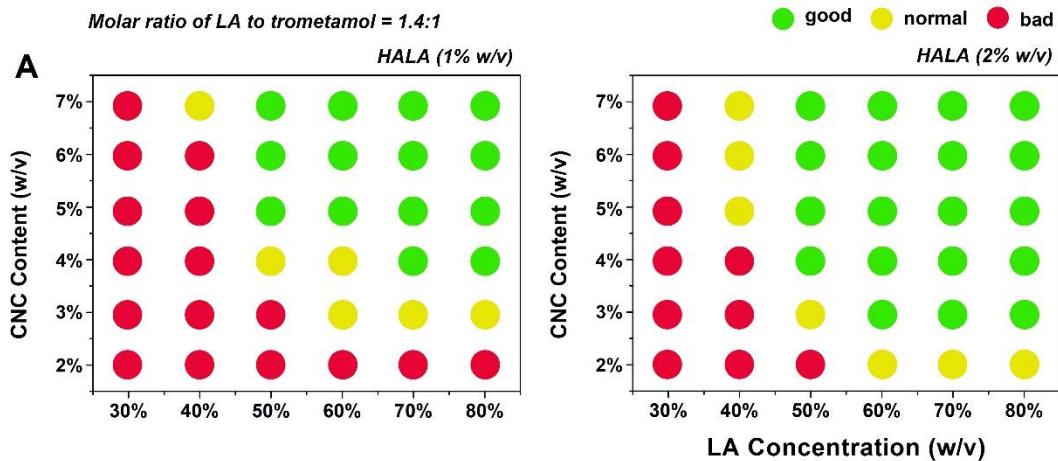


Figure S7. Characterization of CNC. (A) SEM image of CNC (Bar scale=100 μm). (B) Size distribution of CNC in water. Discussion: CNC was planned to be introduced into the hydrogel bandage to form extensive hydrogen bonds with the PLA-HA network. As shown in Figure S5A,B, the CNC used in the present study was similar to a "needle-like" nanoparticle with a length of ~ 200 nm and a width of ~ 10 nm. The particle size of CNC in water measured by DLS showed that the average particle size was ~ 237.02 nm.



B *LA: 50% w/v; trometamol: 30% w/v;*
HALA: 2% w/v; CNC: 5%



Figure S8. Evaluation of printability. (A) Effect of HALA concentration and CNC content on printability. (B) Observation of the ink (LA: 50% w/v; trometamol: 30% w/v; HALA: 2% w/v; CNC: 5%) prepared from non-rapidly-gelled system.

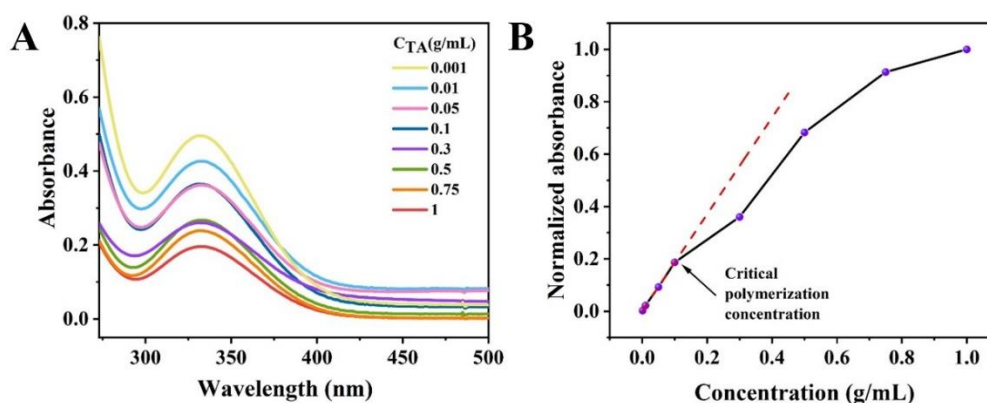


Figure S9. Effect of LA concentration on polymerization in water. (A) UV visible absorption spectra. (B) Normalized absorbance of LA concentration. Discussion: The effect of LA concentration on the polymerization process was studied and showed in Figure S6, by monitoring the UV absorption peak of dithiolane, it was found that when the polymerization concentration was ~ 0.1 g/mL, the relationship between absorbance and concentration deviated from the linear Beer-Lambert line, indicating that the dynamic disulfide bond of LA became close enough to trigger the intermolecular exchange.

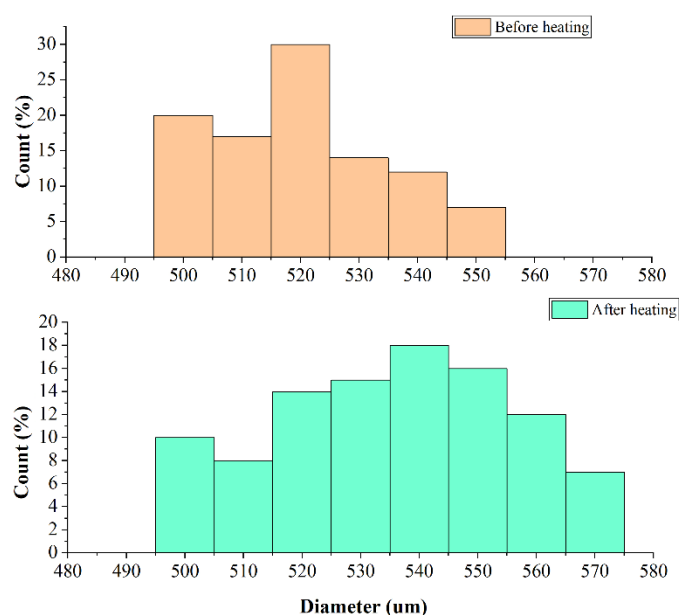


Figure S10. Statistics of the extruded filament diameter before and after 3 hours heating.

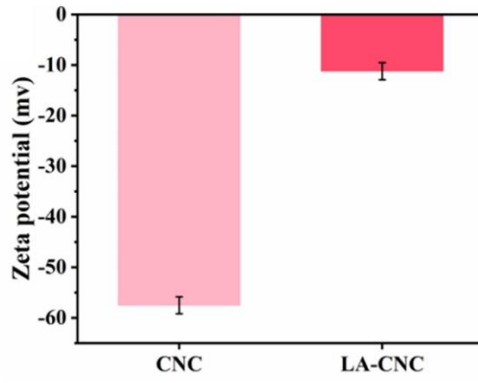


Figure S11. Zeta potential of CNC and LA-CNC.

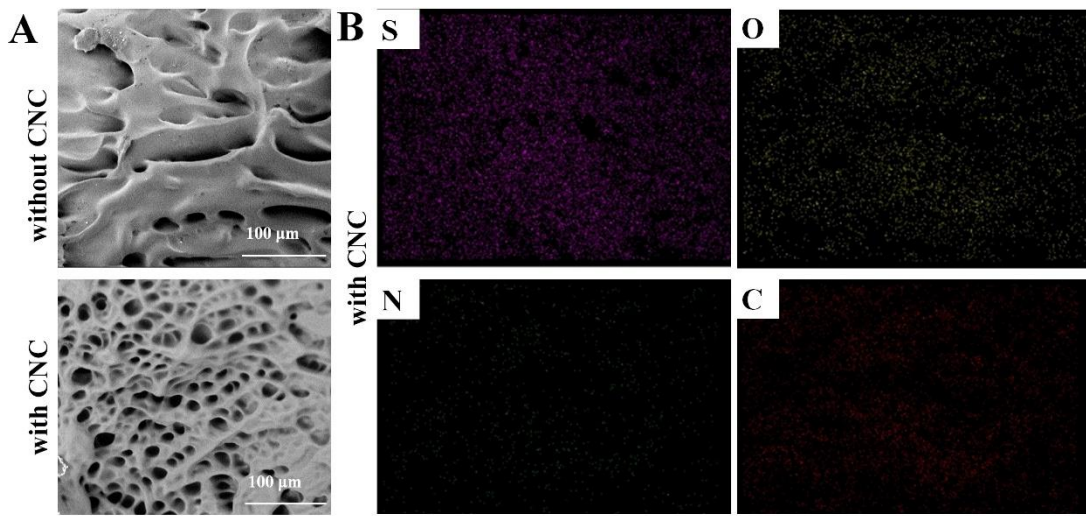


Figure S12. Microstructure of hydrogel bandage with and without CNC. (A) SEM images. (B) EDS images of hydrogel bandage with and without CNC.

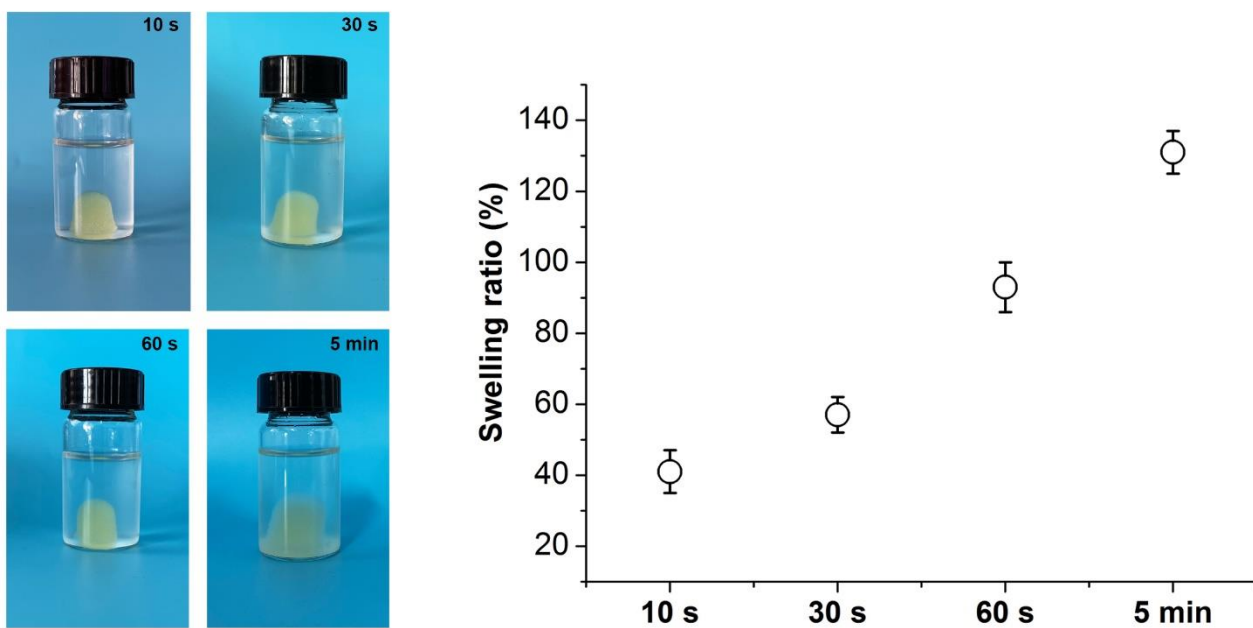


Figure S13. Swelling behavior and swelling ratio of the bandage.

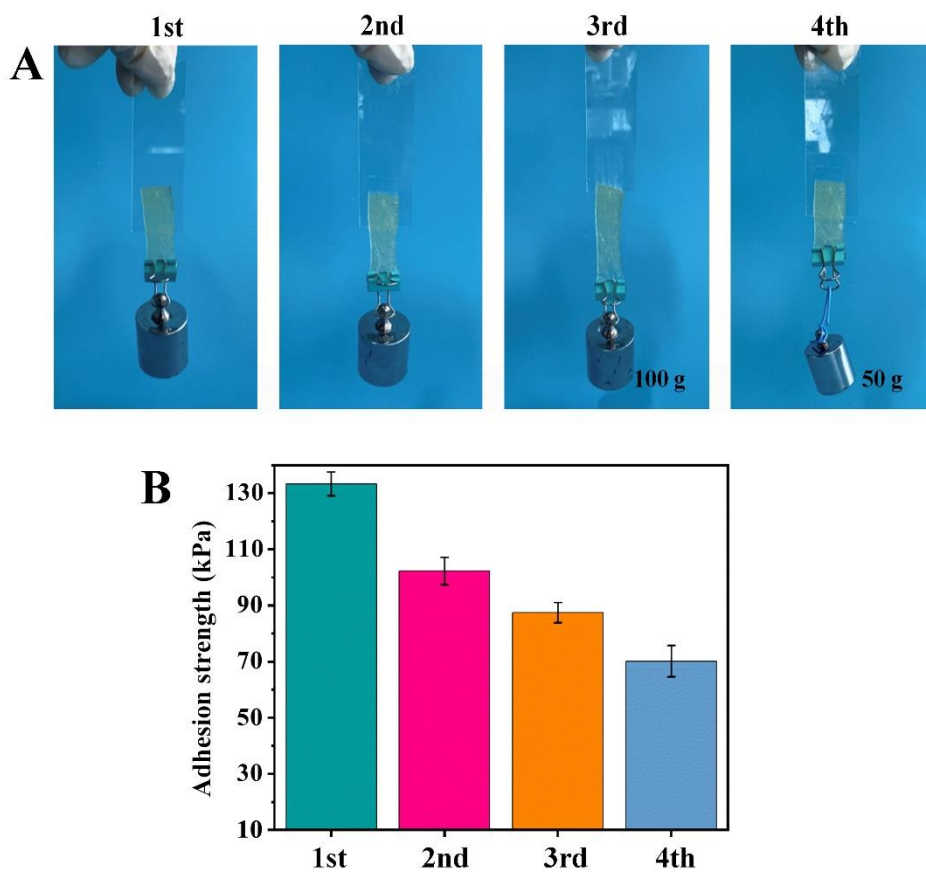


Figure S14. Bandage re-adhesion. (A) Images to show the re-adhesion of the removed hydrogel bandage. (B) Adhesion strength of the re-adhered hydrogel bandage.

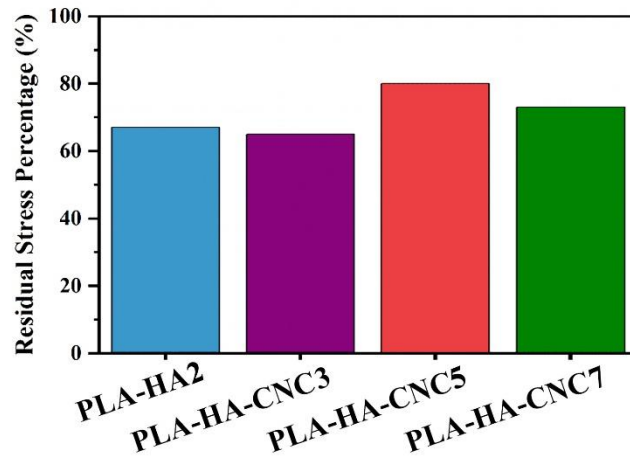


Figure S15. Residual stress percentage of different hydrogels calculated from cyclic compression tests.

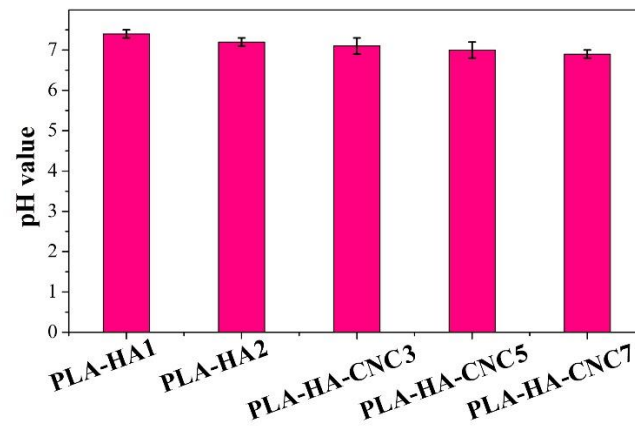


Figure S16. pH value of the hydrogels.

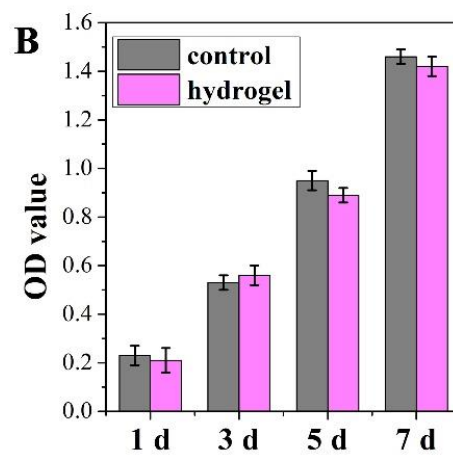
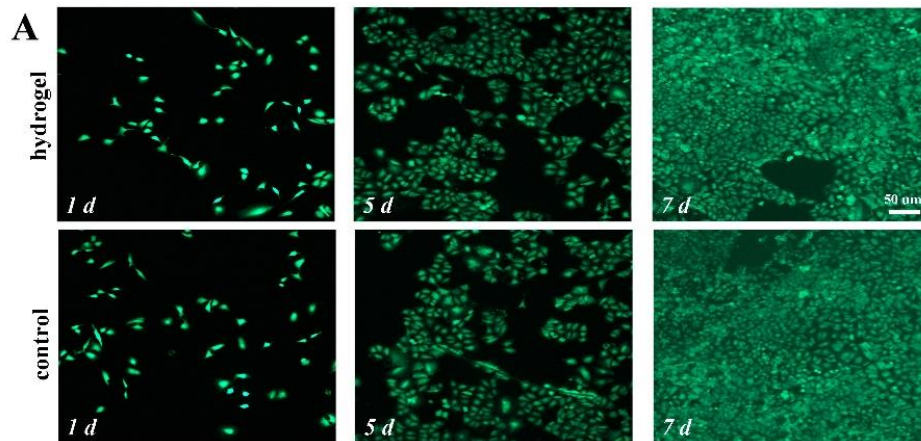


Figure S17. In vitro biocompatibility. (A) Live/dead staining of fibroblasts co-cultured with hydrogel bandage (PLA-HA-CNC2) (Bar scale=50 μ m). (B) OD value to show fibroblasts proliferated after 1, 5, and 7 days culture.

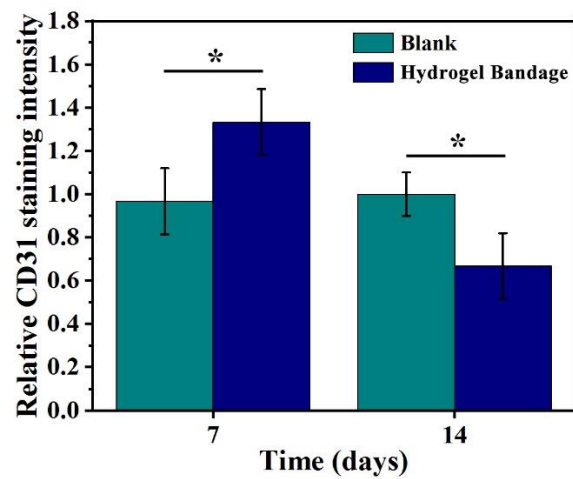


Figure S18. Relative CD31 staining intensity calculated by Image J.

Table S1. DFT calculation results

		$\Delta E(\text{a.u.})$	$\Delta E(\text{eV})$
LA	-1259.58		
Tris	-439.443		
NH ₂ -O	-1699.04	-0.01361	-0.37
NH ₂ -S	-1699.03	-0.00752	-0.205
OH-O	-1699.04	-0.01361	-0.37
OH-S	-1699.04	-0.00997	-0.271

Table S2. Synthesis of HALA

	HA	HALA
M_n	$3.037 \times 10^4 (\pm 2.068\%)$	$1.672 \times 10^4 (\pm 1.480\%)$
M_w	$4.458 \times 10^4 (\pm 0.998\%)$	$2.311 \times 10^4 (\pm 1.079\%)$
M_w/M_n	$1.468 (\pm 2.296\%)$	$1.382 (\pm 1.832\%)$